Soft Matter

Multicomponent Diffusion of Interacting, Nonionic Micelles with Hydrophobic Solutes

Journal:	*Soft Matter*
Manuscript ID	SM-ART-08-2020-001406.R1
Article Type:	Paper
Date Submitted by the Author:	15-Sep-2020
Complete List of Authors:	Alexander, Nathan; University of California Davis, Chemical Engineering Phillips, Ronald; University of California Davis, Chemical Engineering Dungan, Stephanie; University of California Davis, Chemical Engineering; University of California Davis, Food Science and Technology

ARTICLE

Multicomponent Diffusion of Interacting, Nonionic Micelles with Hydrophobic Solutes

Received 00th January 20xx,
Accepted 00th January 20xx

DOI: 10.1039/x0xx00000x

Nathan P. Alexander,[a] Ronald J. Phillips,[a] and Stephanie R. Dungan*[,a,b]

Ternary diffusion coefficient matrices [**D**] were measured using the Taylor dispersion method, for crowded aqueous solutions of decaethylene glycol monododecyl ether ($C_{12}E_{10}$) with either decane or limonene solute. The matrix [**D**], for both systems, was found to be highly non-diagonal, and concentration dependent, over a broad domain of solute to surfactant molar ratios and micelle volume fractions. A recently developed theoretical model, based on Batchelor's theory for gradient diffusion in dilute, polydisperse mixtures of interacting spheres, was simplified by neglecting local polydispersity, and effectively used to predict [**D**] with no adjustable parameters. Even though the model originates from dilute theory, the theoretical results were in surprisingly good agreement with experimental data for concentrated mixtures, with volume fractions up to $\phi \approx 0.47$. In addition, the theory predicts eigenvalues D_- and D_+ that correspond to long-time self and gradient diffusion coefficients, respectively, for monodisperse spheres, in reasonable agreement with experimental data.

1 Introduction

Solute-containing micelle and microemulsion solutions diffuse in response to gradients in chemical potential of either solute or surfactant. Since strong molecular interactions drive self-assembly in these mixtures, the resulting fluxes of solute and surfactant occur in the form of many different species, including free molecular solute, surfactant monomer, dimers, trimers, etc., as well as a distribution of interacting colloidal aggregates with various sizes and shapes. When viewed broadly as a ternary mixture of solute (a), surfactant (s), and solvent, gradient diffusion can be described using the ternary form of Fick's law,

$$-\begin{bmatrix} J_a \\ J_s \end{bmatrix} = \begin{bmatrix} D_{aa} & D_{as} \\ D_{sa} & D_{ss} \end{bmatrix} \begin{bmatrix} \nabla C_a \\ \nabla C_s \end{bmatrix} . \quad (1)$$

In eq 1, the main diffusivities (D_{aa} and D_{ss}) relate the molar flux of solute J_a and surfactant J_s, which are hereby defined relative to the mean volume velocity of the mixture, to their own molar concentration gradients, while the off–diagonal diffusivities (D_{as} and D_{sa}) relate the flux of one component to a concentration gradient of the other. The solvent is excluded from eq 1 because fluxes of three components in a ternary solution are not independent.[1]

Recent studies on multicomponent diffusion in nonionic micellar solutions[2,3] and water–in–oil microemulsions[4,5] indicate strong multicomponent effects, including enhanced surfactant and suppressed solute diffusion down their respective gradients, surfactant diffusion up a solute gradient ($D_{sa} < 0$), and solute diffusion down a surfactant gradient ($D_{as} > 0$). Both cross diffusion effects ($D_{sa} < 0$ and $D_{as} > 0$) were shown capable of establishing buoyancy driven convection (known more generally as double diffusive convection) at the interface between two initially stable ternary microemulsions.[5] Furthermore, suppressed solute diffusion may play a role in limiting the oral absorption rates of hydrophobic drugs, nutrients, and fats when delivered using surfactants to enhance their aqueous solubility.[6,7]

Significant progress has been made toward understanding multicomponent effects in mixtures with nonionic surfactants and solutes.[2–4,8,9] Leaist et al.[4,9] developed a theoretical model for multicomponent diffusion in very dilute solutions with negligible intermicellar interactions. According to this theory, multicomponent effects are driven by solubilization-induced gradients in free molecular solute and surfactant monomer and by counter diffusion of non-interacting micelles with size-dependent Stokes-Einstein mobilities.[4,9] This model was shown to be effective in predicting [**D**] in dilute zwitterionic solutions with relatively hydrophilic alcohols.[9] However, at higher concentrations and in dilute solutions with negligible molecular species, micellar and microemulsion solutions resemble colloidal dispersions, and the influence of particle interactions on [**D**] is expected to play a larger role.

In a series of influential papers,[10–15] Batchelor developed a theory for gradient diffusion in dilute colloidal hard-sphere suspensions, which rigorously accounts for the influence of two-sphere thermodynamic and hydrodynamic interactions (HI). The latter, which are characterized by velocity disturbances transmitted through the viscous liquid between Brownian particles, decay so slowly with interparticle separation distance that they are rarely negligible in colloidal dispersions.[16] However, until recently,[2] HI have been neglected in models that describe multicomponent diffusion in surfactant solutions.

[a] Department of Chemical Engineering, University of California at Davis, Davis, CA 95616 USA. Email: srdungan@ucdavis.edu
[b] Department of Food Science and Technology, University of California at Davis, Davis, CA 95616 USA

The exception is a recent theoretical model by Alexander et al.,[2] developed for nonionic surfactant solutions with negligible molecular species, based on the theory of Batchelor for gradient diffusion in dilute, polydisperse hard-sphere suspensions.[14,15] Hence, this model rigorously accounts for pairwise hydrodynamic and thermodynamic intermicellar interactions, and it successfully predicted $[\mathbf{D}]$ in $C_{12}E_{10}$/decane/water mixtures with no adjustable parameters, up to volume fractions near $\phi = 0.25$.[2]

In the present study, we further test the model of Alexander et al.[2] with new experimental data for aqueous solutions with $C_{12}E_{10}$ micelles and either limonene or decane solutes, at concentrations that approach a micellar solution phase boundary, marking the emergence of a liquid crystalline phase. In addition, we simplify our theoretical equations by neglecting *local* size polydispersity in an effort to make the theory more tractable, and thereby gain physical insight.

2 Materials and Methods

2.1 Materials

Nonionic surfactant decaethylene glycol monododecyl ether ($C_{12}E_{10}$, lot #SLBT1187 or #0000057654, each with a hydroxyl value equal to 92.0 mg/g), and hydrophobic solutes decane and limonene, were all purchased from Sigma-Aldrich and used without modification. Unfiltered, de-ionized water was used to prepare all stock micellar solutions. All mixtures were prepared by volume with aliquots from 100 mL stock solutions, and were allowed to equilibrate overnight at room temperature. Non-ideal changes in volume upon mixing were neglected.

2.2 Taylor dispersion

Ternary diffusion coefficient matrices $[\mathbf{D}]$ were acquired by the Taylor dispersion method,[17,18] using an apparatus and experimental procedure described previously.[2] Data analysis was performed by fitting measured refractive index profiles with the following Taylor dispersion model equation:[19,20]

$$V(t) = V_0 + V_1 t + V_{max}\sqrt{\frac{t_R}{t}}\left\{W exp\left[-\frac{12D_-(t-t_R)^2}{r^2 t}\right] + (1-W) exp\left[-\frac{12D_+(t-t_R)^2}{r^2 t}\right]\right\} . \quad (2)$$

Here, V_0 is the baseline voltage of the detector, V_{max} is the signal voltage when $t = t_R$, and $V_1 t$ captures linear drift in the signal voltage. D_- and D_+ are the eigenvalues of $[\mathbf{D}]$:

$$D_- = \frac{(D_{aa}+D_{ss})}{2} - \frac{\sqrt{(D_{aa}-D_{ss})^2 + 4D_{as}D_{sa}}}{2} \quad (3)$$

$$D_+ = \frac{(D_{aa}+D_{ss})}{2} + \frac{\sqrt{(D_{aa}-D_{ss})^2 + 4D_{as}D_{sa}}}{2} . \quad (4)$$

In eq 2, W is a weighting factor, given by

$$W = \frac{(a+b\alpha_1)\sqrt{D_-}}{(a+b\alpha_1)\sqrt{D_-} + (1-a-b\alpha_1)\sqrt{D_+}} \quad (5)$$

and

$$\alpha_1 = \frac{R_a \Delta C_a}{R_a \Delta C_a + R_s \Delta C_s} \quad (6)$$

$$a = \frac{D_+ - D_{ss} - \frac{R_a}{R_s} D_{as}}{D_+ - D_-} \quad (7)$$

$$b = \frac{D_{ss} + \frac{R_a}{R_s} D_{as} - D_{aa} - \frac{R_s}{R_a} D_{sa}}{D_+ - D_-} . \quad (8)$$

The parameters $R_a = (\partial n/\partial C_a)_{C_s}$ and $R_s = (\partial n/\partial C_s)_{C_a}$ are the refractive index increments with either C_s or C_a held constant, respectively.

In order to acquire the four non-linear fit parameters a, b, D_-, and D_+ of eq 2, two refractive index profiles with two different values for α_1 were fit simultaneously, using non-linear least squares regression performed with Matlab's "patternsearch" algorithm.[21] One profile was generated from a pulse with excess solute ($\alpha_1 \approx 1$) and another from a pulse with excess surfactant ($\alpha_1 \approx 0$). The fit parameters were then used to evaluate $[\mathbf{D}]$ via

$$D_{aa} = D_- + \frac{a(1-a-b)}{b}(D_- - D_+) \quad (9)$$

$$D_{as} = \frac{R_s}{R_a}\frac{a(1-a)}{b}(D_- - D_+) \quad (10)$$

$$D_{sa} = \frac{R_a}{R_s}\frac{(a+b)(1-a-b)}{b}(D_+ - D_-) \quad (11)$$

$$D_{ss} = D_+ + \frac{a(1-a-b)}{b}(D_+ - D_-) . \quad (12)$$

The ratios R_a/R_s in eqs 10 and 11 were evaluated by integrating the refractive index profiles according to $R_a/R_s \approx A_a G_s / A_s G_a$. Here, A_a and A_s are the areas under the dispersion profiles with $\alpha_1 \approx 1$ and $\alpha_1 \approx 0$, respectively, and G_a and G_s are the corresponding detector gain settings. Error bars for the resulting elements of $[\mathbf{D}]$ represent two standard deviations.

3 Results

3.1 Ternary diffusivities and eigenvalues

The Taylor dispersion method was used to measure the ternary diffusion coefficient matrix $[\mathbf{D}]$ at constant temperature T = 23.0 ± 0.3 °C and pressure for aqueous $C_{12}E_{10}$/limonene and $C_{12}E_{10}$/decane mixtures. In Figure 1, $[\mathbf{D}]$ and eigenvalues D_- and D_+ are shown for aqueous solutions of 200mM $C_{12}E_{10}$ with limonene concentrations C_a in the range $0 \le C_a \le 100mM$. The coefficients that comprise $[\mathbf{D}]$ were also measured in $C_{12}E_{10}$/limonene (Figure 2) and $C_{12}E_{10}$/decane (Figure 3) solutions that were diluted with water while maintaining a constant molar ratio of solute to surfactant equal to C_a/C_s = 0.1.

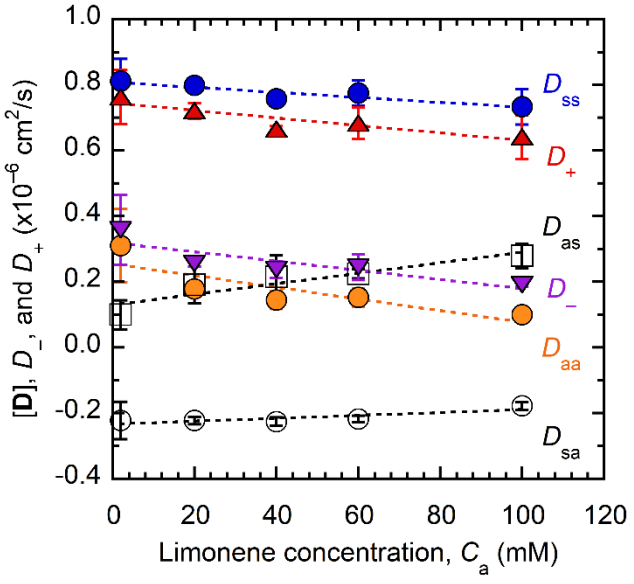

Figure 1. Ternary diffusion coefficients and eigenvalues for aqueous 200mM $C_{12}E_{10}$ (s) + limonene (a) for $C_a/C_s = 0.01$, 0.1, 0.2, 0.3, and 0.5.

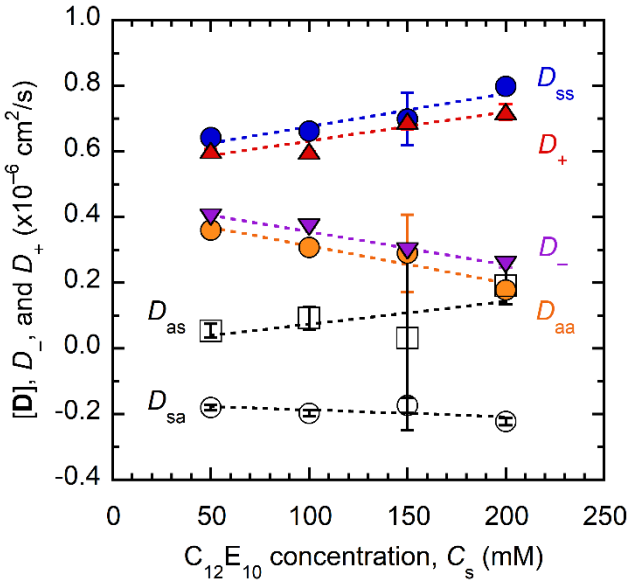

Figure 2. Ternary diffusion coefficients and eigenvalues for aqueous $C_{12}E_{10}$ (s) + limonene (a) with $C_a/C_s = 0.1$.

The critical micelle concentration of $C_{12}E_{10}$ (0.09mM)[22] and the aqueous solubilities of limonene (0.10mM)[23] and decane (3.2×10^{-4}mM)[24] are small compared with the surfactant ($C_s \geq 20mM$) and solute ($C_a \geq 2mM$) concentrations used in this study. Hence, aqueous $C_{12}E_{10}$/limonene and $C_{12}E_{10}$/decane mixtures diffused almost exclusively as solute-containing micelles while surfactant monomer and molecular solute fluxes contributed negligibly to $[\mathbf{D}]$.

Theoretical results for gradient diffusion of colloidal hard spheres by Batchelor[13–15] were derived relative to a volume-fixed reference frame, defined such that the net flux of material volume is zero. Diffusion measurements are generally performed relative to a fixed-laboratory reference frame. However, the lab frame approximates the volume-fixed frame

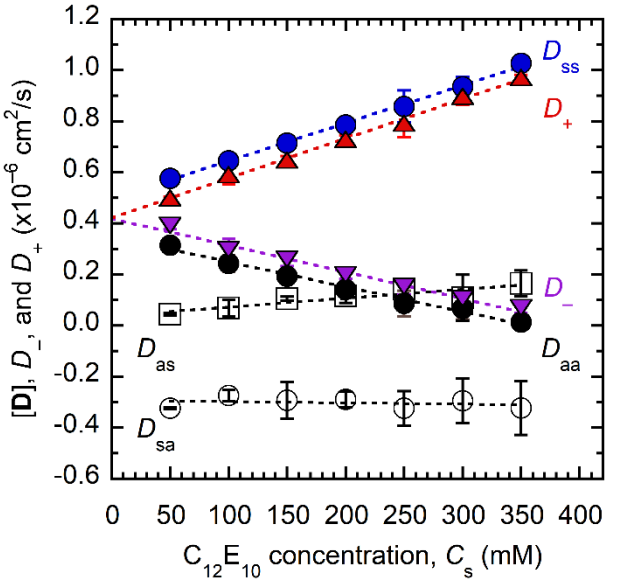

Figure 3. Ternary diffusion coefficients and eigenvalues for aqueous $C_{12}E_{10}$ (s) + decane (a) with $C_a/C_s = 0.1$.

when non-ideal changes in the volume of the solution are negligible upon mixing.[25] That condition is satisfied when either the component molar volumes are constant with composition or when the initial concentration differences, established during the measurement, are made sufficiently small.[25] In this work, we have established small initial concentration differences (5mM) in either the solute or the surfactant in an effort to minimize non-ideal changes in volume upon mixing. As a result, $[\mathbf{D}]$ correspond to the volume-fixed reference frame.

4 Discussion

4.1 Ternary diffusion in $C_{12}E_{10}$/solute/water mixtures

As shown in Figures 1, 2, and 3, the diffusion coefficient matrices $[\mathbf{D}]$, measured via the Taylor dispersion method for both $C_{12}E_{10}$/limonene/water and $C_{12}E_{10}$/decane/water mixtures, are qualitatively similar. Both systems exhibit strong diffusion coupling, including solute diffusion down a surfactant gradient ($D_{as} > 0$) and surfactant diffusion up a solute gradient ($D_{sa} < 0$). Interestingly, the cross diffusivity D_{sa} for both limonene (Figure 2) and decane (Figure 3) is insensitive to surfactant concentration and extrapolates to a nonzero value in the limit as $C_s \to 0$, indicating that this strong coupling effect is weakly influenced by intermicellar interactions. In contrast, the main solute D_{aa} and surfactant D_{ss} diffusivities (Figures 2 and 3), strongly diverge with increasing C_s and are similar to the slow D_- and fast D_+ eigenvalues, respectively, with ($D_{aa} < D_-$) and ($D_{ss} > D_+$) for all mixtures. In Figure 3, D_{aa} (and D_-) fall to near zero with increasing C_s, indicating solute diffusion down its own gradient is nearly arrested at the highest surfactant concentration, $C_s = 350mM$.

4.2 Development of theory

In this section, we further develop a theoretical model introduced in our earlier work,[2] which is based on Batchelor's[14,15] theory for gradient diffusion in polydisperse colloidal mixtures, to describe gradient diffusion in solutions of solute-containing micelles with negligible molecular species. Here, micellar solutions are modeled as polydisperse, colloidal dispersions containing N different particle types, self-assembled from various numbers of solute and surfactant molecules. The molar flux J_i of micelle type i containing n_i solutes and m_i surfactants is defined relative to the mean volume velocity of the mixture and given by the generalized form of Fick's law,

$$-J_i = \sum_{j=1}^{N} D_{ij} \nabla C_j \ . \tag{13}$$

The main micelle diffusivities D_{ii} relate the flux of each micelle species i to its own molar concentration gradient ∇C_i, whereas the micelle cross diffusivities D_{ij} $(j \neq i)$, which accommodate micelle-micelle diffusion coupling, relate the flux of a micelle species i to a concentration gradient in a different micelle species j.

The diffusivities D_{ij} are evaluated using Batchelor's theory for gradient diffusion of polydisperse colloidal particle mixtures,[14]

$$D_{ij} = \frac{D_i^0}{k_B T} \sum_{k=1}^{N} B_{ik} \phi_i \left\{ {\lambda_{ij}}^3 \left(\frac{\partial \mu_k}{\partial \phi_j} \right)_{p,T} + \frac{{\lambda_{ik}}^3}{1-\phi} \sum_{l=1}^{N} {\lambda_{lj}}^3 \phi_l \left(\frac{\partial \mu_l}{\partial \phi_j} \right)_{p,T} \right\} . \tag{14}$$

Here, as applied to our system, D_i^0, B_{ik}, and ϕ_i are the infinite dilution diffusivity, bulk mobility coefficient, and volume fraction of micelle species i. $\phi = \sum_{i=1}^{N} \phi_i$ is the total micelle volume fraction, μ_k is the chemical potential of micelle species k, and $\lambda_{ij} = \left(\frac{V_j}{V_i}\right)^{1/3}$ is a ratio of characteristic lengths, where V_j and V_i are the volumes for a type j and i micelle, respectively.

Neglecting flux contributions from singly dissolved solute and surfactant molecules, the net flux of solute J_a and surfactant J_s are calculated via weighted sums of the micelle species fluxes

$$J_{\mathrm{a}} = \sum_{i=1}^{N} n_i J_i \tag{15}$$

$$J_{\mathrm{s}} = \sum_{i=1}^{N} m_i J_i \ . \tag{16}$$

To derive the diffusivity matrix $[\mathbf{D}]$, one can expand eq 13 with the chain rule and combine the result with eqs 1 and 14–16,

$$D_{\mathrm{aa}} = \sum_{i=1}^{N} \frac{n_i D_i^0}{k_B T} \sum_{j=1}^{N} \sum_{k=1}^{N} B_{ik} \phi_i \left\{ {\lambda_{ij}}^3 \left(\frac{\partial \mu_k}{\partial \phi_j} \right)_{p,T} + \frac{{\lambda_{ik}}^3}{1-\phi} \sum_{l=1}^{N} {\lambda_{lj}}^3 \phi_l \left(\frac{\partial \mu_l}{\partial \phi_j} \right)_{p,T} \right\} \frac{\partial C_j}{\partial C_{\mathrm{a}}} \tag{17}$$

$$D_{\mathrm{as}} = \sum_{i=1}^{N} \frac{n_i D_i^0}{k_B T} \sum_{j=1}^{N} \sum_{k=1}^{N} B_{ik} \phi_i \left\{ {\lambda_{ij}}^3 \left(\frac{\partial \mu_k}{\partial \phi_j} \right)_{p,T} + \frac{{\lambda_{ik}}^3}{1-\phi} \sum_{l=1}^{N} {\lambda_{lj}}^3 \phi_l \left(\frac{\partial \mu_l}{\partial \phi_j} \right)_{p,T} \right\} \frac{\partial C_j}{\partial C_{\mathrm{s}}} \tag{18}$$

$$D_{\mathrm{sa}} = \sum_{i=1}^{N} \frac{m_i D_i^0}{k_B T} \sum_{j=1}^{N} \sum_{k=1}^{N} B_{ik} \phi_i \left\{ {\lambda_{ij}}^3 \left(\frac{\partial \mu_k}{\partial \phi_j} \right)_{p,T} + \frac{{\lambda_{ik}}^3}{1-\phi} \sum_{l=1}^{N} {\lambda_{lj}}^3 \phi_l \left(\frac{\partial \mu_l}{\partial \phi_j} \right)_{p,T} \right\} \frac{\partial C_j}{\partial C_{\mathrm{a}}} \tag{19}$$

$$D_{\mathrm{ss}} = \sum_{i=1}^{N} \frac{m_i D_i^0}{k_B T} \sum_{j=1}^{N} \sum_{k=1}^{N} B_{ik} \phi_i \left\{ {\lambda_{ij}}^3 \left(\frac{\partial \mu_k}{\partial \phi_j} \right)_{p,T} + \frac{{\lambda_{ik}}^3}{1-\phi} \sum_{l=1}^{N} {\lambda_{lj}}^3 \phi_l \left(\frac{\partial \mu_l}{\partial \phi_j} \right)_{p,T} \right\} \frac{\partial C_j}{\partial C_{\mathrm{s}}} \ . \tag{20}$$

Eqs 17–20 define $[\mathbf{D}]$ for a polydisperse solution of micelles with arbitrary shapes, sizes, interaction potentials, and volume fractions. However, for suspensions of arbitrary concentration, the task of evaluating $[\mathbf{D}]$ using this result is formidable.

For dilute mixtures ($\phi \ll 1$), B_{ik} and $\left(\partial \mu_k / \partial \phi_j\right)_{p,T}$, which are generally functions of the species volume fractions $(\phi_1, \phi_2, \ldots, \phi_N)$ and size ratios λ_{ik}, may each be approximated with a series truncated to $O(\phi)$. The series approximations combine with eq 14 to yield,[14]

$$D_{ii} = D_i^0 \left\{ 1 + (\beta + S)\phi_i + \sum_{\substack{k=1 \\ k \neq i}}^{N} K'_{ik} \phi_k \right\} \tag{21}$$

$$\underset{(j \neq i)}{D_{ij}} = D_i^0 \phi_i \left\{ \beta_{ij} \left(\frac{1+\lambda_{ij}}{2} \right)^3 + K''_{ij} \right\} \ . \tag{22}$$

Here, the second osmotic virial coefficients β_{ij} and bulk mobility coefficients K'_{ik} and K''_{ij} depend on the interaction potential between pairs of particles and provide corrections to infinitely dilute particle thermodynamic driving forces and mobilities, respectively. The coefficients $\beta = \beta_{ii}$ and $S = K'_{ii} + K''_{ii}$ account for interactions between identical particles of the same species. Using eqs 21 and 22 in lieu of eq 14, one may derive a theoretical result for $[\mathbf{D}]$ for dilute mixtures of polydisperse micelles with arbitrary shapes, sizes, and pair interactions:

$$D_{\mathrm{aa}} = \sum_{i=1}^{N} n_i D_i^0 \left\{ \left(1 + \sum_{k=1}^{N} K'_{ik} \phi_k \right) \frac{\partial C_i}{\partial C_{\mathrm{a}}} + \phi_i \sum_{j=1}^{N} \left(\beta_{ij} \left(\frac{1+\lambda_{ij}}{2} \right)^3 + K''_{ij} \right) \frac{\partial C_j}{\partial C_{\mathrm{a}}} \right\} \tag{23}$$

$$D_{\mathrm{as}} = \sum_{i=1}^{N} n_i D_i^0 \left\{ \left(1 + \sum_{k=1}^{N} K'_{ik} \phi_k \right) \frac{\partial C_i}{\partial C_{\mathrm{s}}} + \phi_i \sum_{j=1}^{N} \left(\beta_{ij} \left(\frac{1+\lambda_{ij}}{2} \right)^3 + K''_{ij} \right) \frac{\partial C_j}{\partial C_{\mathrm{s}}} \right\} \tag{24}$$

$$D_{\mathrm{sa}} = \sum_{i=1}^{N} m_i D_i^0 \left\{ \left(1 + \sum_{k=1}^{N} K'_{ik} \phi_k \right) \frac{\partial C_i}{\partial C_{\mathrm{a}}} + \phi_i \sum_{j=1}^{N} \left(\beta_{ij} \left(\frac{1+\lambda_{ij}}{2} \right)^3 + K''_{ij} \right) \frac{\partial C_j}{\partial C_{\mathrm{a}}} \right\} \quad (25)$$

$$D_{\mathrm{ss}} = \sum_{i=1}^{N} m_i D_i^0 \left\{ \left(1 + \sum_{k=1}^{N} K'_{ik} \phi_k \right) \frac{\partial C_i}{\partial C_{\mathrm{s}}} + \phi_i \sum_{j=1}^{N} \left(\beta_{ij} \left(\frac{1+\lambda_{ij}}{2} \right)^3 + K''_{ij} \right) \frac{\partial C_j}{\partial C_{\mathrm{s}}} \right\} . \quad (26)$$

In order to calculate $[\mathbf{D}]$ using eqs 23–26, the coefficients β_{ij}, K'_{ik}, and K''_{ij}, as well as the micelle distribution function, must be known. For mixtures of particles that interact as hard spheres, the virial coefficients are given by,[26]

$$\beta_{ij} = 8 \ . \quad (27)$$

Relations from Batchelor[15] provide estimates for the bulk mobility coefficients,

$$K'_{ik} = \frac{-2.5}{1 + 0.16\lambda_{ik}} , \quad (28)$$

and

$$K''_{ij} = \frac{\lambda_{ij}^2}{1+\lambda_{ij}^3} - \left(\lambda_{ij}^2 + 3\lambda_{ij} + 1 \right) , \quad (29)$$

which are accurate to within 5% of numerical calculations for $\frac{1}{8} \leq \lambda_{ij} \leq 8$.

Previously,[2] eqs 21–29 were successfully used to predict $[\mathbf{D}]$ for $C_{12}E_{10}$/decane/water mixtures. In that study, the distribution of micelle species was assumed to obey a Poisson distribution with a mean, variance, and higher moments dependent on the average number of solubilizate molecules per micelle $\bar{n} = C_a/C_s\,\bar{m}$, where $\bar{m}$ is the average micelle aggregation number and the overbar indicates averages weighted by the micelle distribution function. As a result, the moments of the Poisson varied locally with composition along solute and/or surfactant concentration gradients.

However, our previous dynamic light scattering results indicate that decane-containing $C_{12}E_{10}$ micelles in water are narrowly polydisperse with a small relative standard deviation $\sigma_R < 0.1$.[2] Hence, in this work, local polydispersity and the higher moments are neglected, and the micelle distribution is defined using a Kronecker delta with a composition dependent mean:

$$C_i = \frac{C_s}{\bar{m}} \delta_{ii^*} = \begin{Bmatrix} \frac{C_s}{\bar{m}} \ when\ i = i^* \\ 0 \ when\ i \neq i^* \end{Bmatrix} . \quad (30)$$

Here, i^* designates a micelle type with $\bar{n}$ solutes, $\bar{m}$ surfactants, radius R_{i^*}, and a local concentration equal to $C_s/\bar{m}$. Using the delta distribution $C_i = C_s/\bar{m}\,\delta_{ii^*}$, eqs 23–26 may be simplified to (see Appendix A)

$$\frac{D_{\mathrm{aa}}}{D_{i^*}^0} = 1 + K'\phi - M\left(\phi, \frac{C_a}{C_s}\right) \quad (31)$$

$$\frac{D_{\mathrm{as}}}{D_{i^*}^0} = \frac{C_a}{C_s}\left\{ (\beta + K'')\phi + M\left(\phi, \frac{C_a}{C_s}\right) \right\} \quad (32)$$

$$\frac{D_{\mathrm{sa}}}{D_{i^*}^0} = -\frac{C_s}{C_a} M\left(\phi, \frac{C_a}{C_s}\right) \quad (33)$$

$$\frac{D_{\mathrm{ss}}}{D_{i^*}^0} = 1 + (\beta + S)\phi + M\left(\phi, \frac{C_a}{C_s}\right) . \quad (34)$$

The function $M\left(\phi, \frac{C_a}{C_s}\right)$ is given by

$$M\left(\phi, \frac{C_a}{C_s}\right) = \frac{\partial ln R_{i^*}}{\partial ln C_a}(1 + \gamma\phi) - (\beta + K'')\phi_a \ , \quad (35)$$

where $\phi_a = C_a N_A V_a$ is the solute volume fraction, N_A is Avogadro's number, V_a is the molecular volume of the solute, and the parameter γ is evaluated according to

$$\gamma = \left(\frac{3}{2}\beta + K' + 3K'' \right) - \left\{ \frac{d(K'' - K')}{d\lambda} \right\}_{\lambda=1} . \quad (36)$$

$D_{i^*}^0$ is calculated using the Stokes-Einstein equation

$$D_{i^*}^0 = \frac{k_B T}{6\pi\eta R_{i^*}} \ , \quad (37)$$

the volume fraction ϕ is determined using

$$\phi = N_A \frac{C_s}{\bar{m}} \frac{4}{3} \pi R_{i^*}^3 , \quad (38)$$

and the aggregation number can be evaluated using a micelle volume balance with $\bar{n} = C_a/C_s\,\bar{m}$,

$$\bar{m} = \frac{\frac{4}{3}\pi R_{i^*}^3}{\frac{C_a}{C_s} V_a + V_s + n_H V_w} . \quad (39)$$

Here, V_s, V_a, and V_w are the respective molecular volumes of a dry molecule of $C_{12}E_{10}$, solute, and water, and the hydration index n_H is the number of bound water molecules per surfactant molecule.

Note, according to eq B.1 in Appendix B, the derivative $\frac{\partial ln R_{i^*}}{\partial ln C_a}$ is a univariate function of C_a/C_s. Furthermore, the solute volume fraction ϕ_a can be rewritten using eqs 38 and 39 to yield $\phi_a = \frac{C_a}{C_s}\left(\frac{V_a}{\frac{C_a}{C_s}V_a + V_s + n_H V_w} \right)\phi$. Thus, the function $M\left(\phi, \frac{C_a}{C_s}\right)$, defined by eq 35, is dependent on C_a/C_s and ϕ.

The parameters n_H and R_{i^*} are experimentally accessible as functions of C_a/C_s via light scattering measurements extrapolated to infinite dilution, while data at higher concentrations indicates the particle interaction potential. For solutions of micelles that interact as hard spheres, $\beta = 8$ and exact calculations by Batchelor[12,15] provide $K' = -2.10$, $K'' = -4.45$, $S = K' + K'' = -6.55$, and $\gamma = 1.25$ (see Appendix A).

The remaining parameters are determined using eqs 37–39. As a result, the model defined by eqs 31–39 has no adjustable parameters.

Theoretical predictions for the eigenvalues of $[\mathbf{D}]$ may be determined using eqs 3, 4, and 31–34,

$$\frac{D_-}{D_{i^*}^0} = 1 + K'\phi \tag{40}$$

$$\frac{D_+}{D_{i^*}^0} = 1 + (\beta + S)\phi \ . \tag{41}$$

Remarkably, eqs 40 and 41 indicate that D_- and D_+ correspond to self and gradient diffusion coefficients, respectively, for colloidal suspensions of monodisperse spheres, even though strong multicomponent diffusion effects may cause $[\mathbf{D}]$ to be highly non-diagonal.

4.3 Label and tracer limits for $[\mathbf{D}]$

It is insightful to examine $[\mathbf{D}]$ for the special case in which a solute behaves as a volume-less label in a solution of equally sized micelles with $\phi_a = 0$, $\bar{m} = m_0$, $R_{i^*} = R_0$, and $D_{i^*}^0 = D^0$ where m_0, R_0, and D^0 are the solute-free micelle aggregation number, radius, and infinite dilution diffusivity, respectively. Here, micelles containing various numbers of solute labels diffuse with an average size and aggregation number that do not vary along solute or surfactant gradients. As a result, $M\left(\phi, \frac{C_a}{C_s}\right) = 0$, and eqs 31–34 simplify to

$$\frac{D_{\mathrm{aa}}}{D^0} = 1 + K'\phi \tag{42}$$

$$\frac{D_{\mathrm{as}}}{D^0} = \frac{C_{\mathrm{a}}}{C_{\mathrm{s}}}(\beta + K'')\phi \tag{43}$$

$$D_{\mathrm{sa}} = 0 \tag{44}$$

$$\frac{D_{\mathrm{ss}}}{D^0} = 1 + (\beta + S)\phi \ . \tag{45}$$

In this case, solute diffuses down its own gradient at a rate determined by the micelle self diffusion coefficient, according to eq 42, and surfactant diffuses down a surfactant gradient according to the micelle gradient diffusion coefficient, given by eq 45. Furthermore, solute is carried within micelles down a surfactant gradient according to eq 43, while D_{sa} is predicted to equal zero. Eqs 42–45 describe 'baseline' multicomponent effects, common to ternary mixtures with any hydrophobic solute. Comparison of eqs 31–34 with eqs 42–45 indicate that the unique properties of a particular solute (i.e. its size, polarity, etc.) may affect $[\mathbf{D}]$ through the function $M\left(\phi, \frac{C_a}{C_s}\right)$ and the Stokes-Einstein diffusivity $D_{i^*}^0$. Per eqs 35–37, solubilizate alters the microstructure of a solution through $M\left(\phi, \frac{C_a}{C_s}\right)$ and $D_{i^*}^0$ by shifting the average micelle size R_{i^*}, which it may accomplish by occupying volume and by changing the average micelle aggregation number.

Some appreciation for the implications of eqs 42–45 can be gained by considering their predictions in different physical conditions. In the limit of infinite dilution, there are no off–diagonal elements of $[\mathbf{D}]$, and both of the diagonal terms D_{aa} and D_{ss} equal the solute-free Stokes-Einstein diffusivity D^0. Hence, in the absence of micelle-micelle interactions, solute and surfactant fluxes are both proportional to gradients in their own concentrations, and independent of the other. Next, consider a case where there is no gradient in surfactant concentration, but there is a gradient in solute concentration. The role of solute is only to label the micelles. The solute flux, therefore, must be governed by the self diffusion coefficient that describes the random walk of identical micelles in the absence of any imposed gradient in micelle concentration. That coefficient is given by eq 42. By contrast, if solute and surfactant gradients are imposed with the molar ratio C_a/C_s held fixed, so that every micelle along the gradient has the same amount of solute with the same radius and aggregation number, then clearly the solute (and surfactant) flux is governed by the gradient diffusion coefficient of the micelles. Indeed, using eqs 1, 42–45 (or, more generally, using eqs 31–34), and the constraint $\nabla(C_a/C_s) = 0$, one can show that $[\mathbf{D}]$ degenerates to the micelle gradient diffusion coefficient according to $[\mathbf{D}] = D^0\{1 + (\beta + S)\phi\}[\mathbf{I}]$, where $[\mathbf{I}]$ is the identity matrix. Absent any such constraints, even in a solution with no gradient in solute concentration, micelle-micelle interactions can yield a gradient in solute chemical potential that drives a solute flux.

We now examine $[\mathbf{D}]$ for a different special case in which solute retains its identity but is present in trace amounts, corresponding to the limit $C_a/C_s \to 0$. In this limit, $M\left(\phi, \frac{C_a}{C_s}\right) \to 0$ and $D_{i^*}^0 \to D^0$, so that eqs 31–34 become (see Appendix B)

$$\frac{D_{\mathrm{aa}}}{D^0} = 1 + K'\phi \tag{46}$$

$$D_{\mathrm{as}} = 0 \tag{47}$$

$$\frac{D_{\mathrm{sa}}}{D^0} = -\frac{a_1}{R_0}(1 + \gamma\phi) + (\beta + K'')\left(\frac{V_{\mathrm{a}}}{V_{\mathrm{s}} + n_{\mathrm{H}}V_{\mathrm{w}}}\right)\phi \tag{48}$$

$$\frac{D_{\mathrm{ss}}}{D^0} = 1 + (\beta + S)\phi \ . \tag{49}$$

Here, a_1 may be interpreted as a micelle growth rate, indicating how strongly the average micelle radius varies with the molar ratio C_a/C_s (see eq A.21). Eqs 46 and 49 indicate that solute and surfactant diffuse down their respective gradients according to self and gradient diffusion coefficients of monodisperse spheres, which is the same behaviour predicted by eqs 42 and 45 when solute was assumed to behave as a label. Furthermore, solutes with larger growth rates a_1 drive stronger uphill surfactant fluxes ($D_{\mathrm{sa}} < 0$) per eq 48 and surfactant gradients do not drive solute fluxes per eq 47 when micelles carry only trace amounts of solute.

4.4 Comparison with experimental data

Theoretical predictions for $[\mathbf{D}]$ for aqueous $C_{12}E_{10}$/decane and $C_{12}E_{10}$/limonene mixtures were calculated using eqs 31–39 with V_{a} = 0.32 nm^{-3} (decane) or 0.26 nm^{-3} (limonene), V_{s} = 0.99 nm^{-3}, V_{w} = 0.03 nm^{-3}, $\beta = 8$, $K' = -2.10$, $K'' = -4.45$, $S = K' + K'' = -6.55$, and $\gamma = 1.25$. The remaining parameters, n_{H} and R_{i^*}, were evaluated in accordance with our light

scattering results,[2] which indicate n_{H} = 40 and $R_{i^*} = a_1 \frac{C_a}{C_s} + R_0$ with a solute-free micelle radius R_0 = 3.78 nm and growth rate a_1 = 2.42 nm (decane) or 1.56 nm (limonene). The growth rate for limonene was determined from currently unpublished dynamic light scattering data, following the same procedure used to acquire the decane value.[2] In Figure 4A,B, theoretical results and experimental data for $[\mathbf{D}]$ are plotted as a function of C_a/C_s and ϕ for concentrated solutions of $C_{12}E_{10}$ micelles with either limonene (Figure 4A) or decane (Figure 4B), respectively.

Overall, the theoretical results are in good agreement with the experimental values over the entire volume fraction and molar ratio domains, which is surprising given that the model is based on Batchelor's theory for dilute particle mixtures, and has no adjustable parameters. As shown, the model captures cross diffusion coupling, including solute diffusion down a surfactant gradient ($D_{as} > 0$) and surfactant diffusion up a solute gradient ($D_{sa} < 0$). Furthermore, in Figure 4B, enhanced surfactant (D_{ss}) and suppressed solute (D_{aa}) diffusion down their respective gradients with increasing ϕ are also accurately predicted.

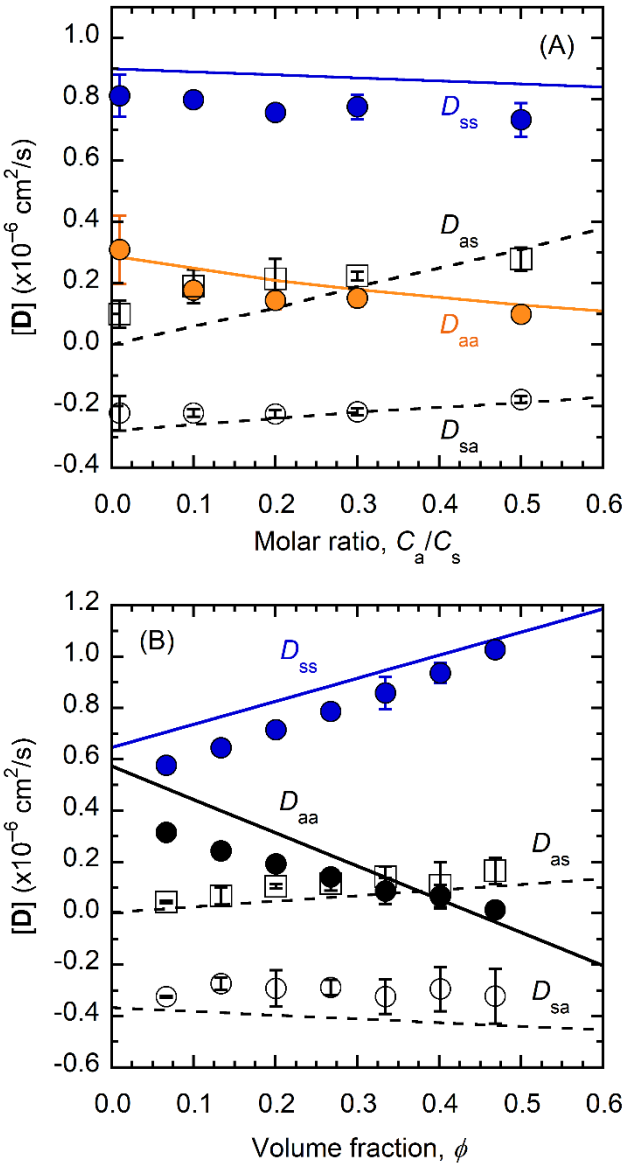

Figure 4. Ternary diffusion coefficients for (A) aqueous 200mM $C_{12}E_{10}$ (s) + limonene (a) and (B) aqueous $C_{12}E_{10}$ (s) + decane (a) with $C_a/C_s = 0.1$. Theoretical predictions for [**D**], shown as solid and dashed lines, were calculated using eqs 31–39.

As noted by others,[27,28] Batchelor's dilute theory for gradient diffusion in monodisperse hard sphere dispersions agrees well with numerical results[28,29] for concentrated particle mixtures up to $\phi \approx 0.4$, suggesting a near cancellation of higher order, many-body hydrodynamic and thermodynamic virial contributions. We note that, according to eqs 31–36, thermodynamic and hydrodynamic virial coefficients are nearly always present together as a sum, perhaps with the exception of K' in eq 31. Hence, cancellation similar to that hypothesized for binary gradient diffusion may occur in $[\mathbf{D}]$, thereby extending the domain over which our dilute multicomponent theory, defined by eqs 31–39, provides accurate results.

Eqs 31–34 were derived assuming negligibly polydisperse, spherical micelles that may vary in R_{i^*} and $\bar{m}$ with C_a/C_s but not with ϕ (see appendix A, eqs A.21 and A.22). Hence, good agreement between our theoretical and experimental values for $[\mathbf{D}]$ for mixtures comprising $C_{12}E_{10}$ micelles with either decane or limonene solute provides evidence that, to a good approximation, these micelles behave as locally monodisperse hard spheres that do not significantly change in size or shape with respect to surfactant concentration, while holding the molar ratio constant, over the entire volume fraction and molar ratio domain explored in this study. This result is consistent with literature[2,30–37] on the morphological behavior of micelles formed with $C_{12}E_{10}$ or related $C_{12}E_n$ surfactants, at least over a portion of the micellar solution region of their respective phase diagrams. Furthermore, the large size of $C_{12}E_{10}$'s headgroup suggests that it should form spherical micellar aggregates over a significant temperature-composition domain.[30,31]

At temperatures sufficiently far below the cloud point curve, hard-sphere behaviour and a weak dependence of micelle size with respect to surfactant concentration have been reported for mixtures of $C_{12}E_6$/water,[35] $C_{12}E_8$/water,[35] $C_{12}E_{10}$/water,[2] $C_{12}E_{10}$/decane/water,[2] and $C_{12}E_5$/decane/water.[36,37] The latter system is particularly interesting, since light scattering and cryo-TEM data for $C_{12}E_5$/water indicate the presence of worm-like micelles that grow and form branched micellar networks with increasing surfactant concentration for dilute mixtures at temperatures as low as 8 °C.[38] However, when loaded to capacity with decane at significantly higher temperature (23.5 °C), decane-containing $C_{12}E_5$ micelles are reported to behave as nearly ϕ-independent hard spheres over a large volume fraction domain.[36,37] Hence, it is plausible that hard sphere theory could be applicable to ternary mixtures comprising a variety of nonionic surfactants and hydrophobic solutes, especially for nonionic surfactants with large headgroups relative to their hydrocarbon tails,[30,31] or when heavily loaded with solute.

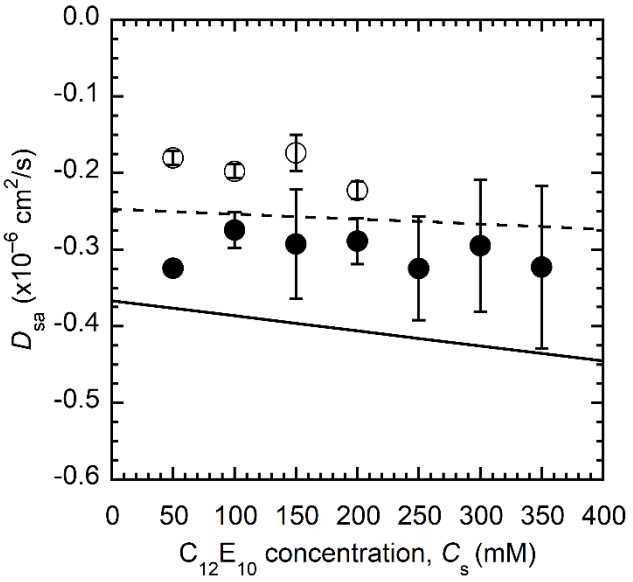

Figure 5. Cross diffusion coefficients D_{sa} for aqueous $C_{12}E_{10}$/decane (closed circles) and $C_{12}E_{10}$/limonene (open circles) with $C_a/C_s = 0.1$. Theoretical predictions for D_{sa} were calculated using eqs 33 and 35–38 and are indicated by solid and dashed lines for mixtures with decane and limonene, respectively.

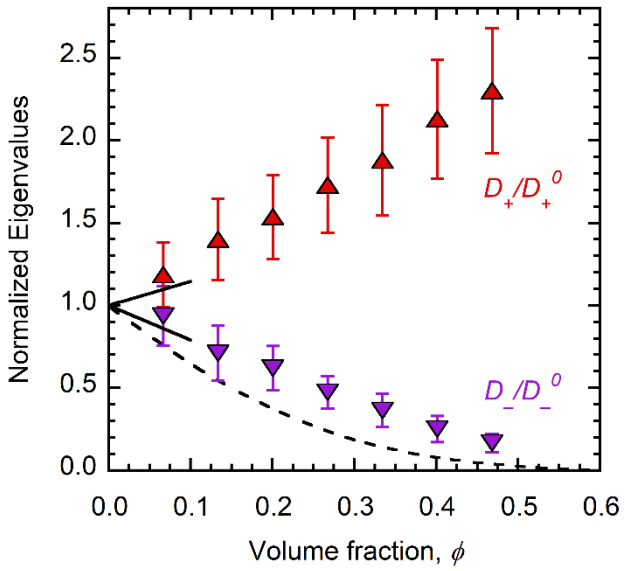

Figure 6. Normalized eigenvalues for aqueous $C_{12}E_{10}$ (s) + decane (a) with $C_a/C_s = 0.1$. Monodisperse hard sphere theory by Batchelor[13–15] and Brady[41] are shown as solid and dashed lines, respectively. Error bars indicate 95% confidence intervals.

Predictions for $[\mathbf{D}]$ in the solute tracer limit (eqs 46–49) indicate that $[\mathbf{D}]$ varies with solute type mainly through D_{sa} at low molar ratios. Hence, in order to compare $[\mathbf{D}]$ for different solutes, experimental values for D_{sa} versus C_s for aqueous $C_{12}E_{10}$/decane and $C_{12}E_{10}$/limonene mixtures with $C_a/C_s = 0.1$ are presented in Figure 5, superimposed over theoretical predictions (solid and dashed lines). As shown, D_{sa} values for $C_{12}E_{10}$ micelles with decane are greater in magnitude relative to those with limonene, suggesting that solutes with stronger growth rates a_1 drive stronger uphill surfactant fluxes.

According to solubilization theory,[39,40] micelle growth rates vary with the size and polarity of the solubilizate. Solubilization increases the interfacial area and alters the composition of the micelle core, both of which affect the core-shell interfacial energy of the micelle, driving changes in the aggregation number that affect micelle size. Small solubilizates with relatively high polarities, such as limonene, inflict a smaller interfacial energy penalty when solubilized, driving a smaller increase in the aggregation number, relative to larger, less polar solutes, such as decane. As a result, $C_{12}E_{10}$ micelles with limonene are expected to have a smaller growth rate and weaker cross diffusion coupling than those with decane, which is supported by the data shown in Figure 5, and is consistent with predictions for D_{sa} in the tracer limit according to eq 48.

In Figure 6, measurements for the eigenvalues D_- and D_+ for $C_{12}E_{10}$/decane/water mixtures with $C_a/C_s = 0.1$ are normalized with their respective values at infinite dilution (D_-^0 and D_+^0) and plotted as a function of ϕ. The experimental data are superimposed over dilute theory by Batchelor[13–15] (solid lines) for gradient and long-time self diffusion of monodisperse hard spheres. In addition, theory by Brady[41] (dashed line), for long-time self diffusion in concentrated monodisperse hard-sphere suspensions, is also shown. Here, Batchelor's dilute theory is expected to be more accurate for $\phi \ll 1$, while the theory by Brady provides an approximate result over the entire concentration domain up to the random close packing fraction for hard spheres ($\phi \approx 0.63$). As shown, the normalized eigenvalues D_-/D_-^0 and D_+/D_+^0 diverge with increasing ϕ, with slopes over the entire range of volume fractions equal to -1.9 ± 0.2 and 2.7 ± 0.1, respectively. These values are in reasonable agreement with predictions by Batchelor[13–15] for long-time self (-2.10) and gradient (1.45) diffusion of monodisperse hard spheres, supporting our theoretical predictions given by eqs 40 and 41.

5 Conclusions

Interactions between nonionic micelles in concentrated aqueous $C_{12}E_{10}$/decane and $C_{12}E_{10}$/limonene mixtures are shown to strongly affect the ternary diffusion coefficient matrices $[\mathbf{D}]$ for both systems. Hence, theoretical predictions for $[\mathbf{D}]$ that do not account for both thermodynamic and hydrodynamic intermicellar interactions may be misleading. A theoretical model developed previously, based on the rigorous theory by Bachelor for dilute, polydisperse colloidal hard spheres, was simplified by neglecting local size polydispersity, and was effectively used to predict $[\mathbf{D}]$ for both micellar systems with no adjustable parameters. Furthermore, the theoretical predictions are surprisingly accurate far beyond the dilute regime, up to concentrations approaching a phase boundary. Lastly, despite strong multicomponent diffusion effects, the fast D_+ and slow D_- eigenvalues of $[\mathbf{D}]$ for aqueous $C_{12}E_{10}$/decane mixtures correspond to gradient and self diffusion coefficients for monodisperse hard sphere dispersions.

Conflicts of interest

There are no conflicts of interest to declare.

Appendix A: Derivation of $[\mathbf{D}]$ for dilute mixtures of spherical micelles with negligible polydispersity

In this section, we provide a detailed derivation of D_{aa} in eq 31, starting from eq 23. Eqs 32–34 may be derived by an analogous approach, yielding the complete matrix $[\mathbf{D}]$. We begin with eq 23,

$$D_{\mathrm{aa}} = \sum_{i=1}^{N} n_i D_i^0 \left\{ \left(1 + \sum_{k=1}^{N} K'_{ik}\phi_k \right) \frac{\partial C_i}{\partial C_{\mathrm{a}}} + \phi_i \sum_{j=1}^{N} \left(\beta_{ij} \left(\frac{1+\lambda_{ij}}{2} \right)^3 + K''_{ij} \right) \frac{\partial C_j}{\partial C_{\mathrm{a}}} \right\} . \quad (A.1)$$

In eq A.1, C_i and $\phi_i = C_i N_A V_i$ are the only functions of C_{a} and C_{s}, permitting rearrangement to the following amenable form,

$$D_{\mathrm{aa}} = \sum_{i=1}^{N} \frac{\partial \left(n_i D_i^0 C_i \right)}{\partial C_a} \left(1 + \sum_{k=1}^{N} K'_{ik}\phi_k \right) + \sum_{i=1}^{N} n_i D_i^0 \phi_i \frac{\partial}{\partial C_{\mathrm{a}}} \sum_{j=1}^{N} \left\{ \beta_{ij} \left(\frac{1+\lambda_{ij}}{2} \right)^3 + K''_{ij} \right\} C_j . \quad (A.2)$$

For micelle distributions that are monomodal and narrow, reasonable approximations for the species concentrations C_i, and volume fractions ϕ_i, can be defined using a Kronecker delta distribution function (see eq 30), so that $C_i = C_s/\overline{m}\,\delta_{ii^*}$ and $\phi_i = C_s/\overline{m}\,N_A V_i \delta_{ii^*}$. According to this definition, C_i is nonzero only when the index $i = i^*$, which denotes a micelle type representative of the distribution mean and characterized as having $\overline{n}$ solutes, $\overline{m}$ surfactants, radius R_{i^*}, and concentration $C_s/\overline{m}$, all of which are functions of composition (C_a and C_s). Inserting the Kronecker distribution into eq A.2 yields,

$$D_{\mathrm{aa}} = \sum_{i=1}^{N} \frac{\partial \left(n_i D_i^0 \frac{C_s}{\overline{m}} \delta_{ii^*} \right)}{\partial C_a} \left(1 + \sum_{k=1}^{N} K'_{ik} \frac{C_s}{\overline{m}} N_A V_k \delta_{ki^*} \right) + \sum_{i=1}^{N} n_i D_i^0 \frac{C_s}{\overline{m}} N_A V_i \delta_{ii^*} \frac{\partial}{\partial C_{\mathrm{a}}} \left\{ \sum_{j=1}^{N} \left\{ \beta_{ij} \left(\frac{1+\lambda_{ij}}{2} \right)^3 + K''_{ij} \right\} \frac{C_s}{\overline{m}} \delta_{ji^*} \right\} . \quad (A.3)$$

Using the sifting property, which selects the micelle type i^* from a set of N different micelle types, with equations $\phi = C_s/\overline{m}\,N_A V_{i^*}$ and $C_a = \overline{n}/\overline{m}\,C_s$, the summations over k and j in eq A.3 are evaluated to give

$$D_{\mathrm{aa}} = \sum_{i=1}^{N} \frac{\partial \left(n_i D_i^0 \frac{C_s}{\overline{m}} \delta_{ii^*} \right)}{\partial C_a} (1 + K'_{ii^*}\phi) + \sum_{i=1}^{N} n_i D_i^0 \frac{C_s}{\overline{m}} N_A V_i \delta_{ii^*} \frac{\partial}{\partial C_{\mathrm{a}}} \left\{ \left\{ \beta_{ii^*} \left(\frac{1+\lambda_{ii^*}}{2} \right)^3 + K''_{ii^*} \right\} \frac{C_s}{\overline{m}} \right\} . \quad (A.4)$$

The product rule is used to rearrange the first summation in eq A.4,

$$\sum_{i=1}^{N} \frac{\partial \left(n_i D_i^0 \frac{C_s}{\overline{m}} \delta_{ii^*} \right)}{\partial C_a} (1 + K'_{ii^*}\phi) = \sum_{i=1}^{N} \left\{ \frac{\partial}{\partial C_a} \left\{ n_i D_i^0 \frac{C_s}{\overline{m}} \delta_{ii^*} (1 + K'_{ii^*}\phi) \right\} - n_i D_i^0 \frac{C_s}{\overline{m}} \delta_{ii^*} \frac{\partial (K'_{ii^*}\phi)}{\partial C_a} \right\} . \quad (A.5)$$

The i summation on the right side of eq A.5 is evaluated using the sifting property, $\phi = C_s/\overline{m}\,N_A V_{i^*}$, and $C_a = \overline{n}/\overline{m}\,C_s$,

$$\sum_{i=1}^{N} \frac{\partial \left(n_i D_i^0 \frac{C_s}{\overline{m}} \delta_{ii^*} \right)}{\partial C_a} (1 + K'_{ii^*}\phi) = \frac{\partial}{\partial C_a} \left\{ C_a D_{i^*}^0 (1 + K'_{i^*i^*}\phi) \right\} - C_a D_{i^*}^0 \left\{ \frac{\partial (K'_{ii^*}\phi)}{\partial C_a} \right\}_{i=i^*} . \quad (A.6)$$

Here, $K'_{i^*i^*}$ is a constant and the derivatives in eq A.6 are expanded to provide,

$$\sum_{i=1}^{N} \frac{\partial \left(n_i D_i^0 \frac{C_s}{\overline{m}} \delta_{ii^*} \right)}{\partial C_a} (1 + K'_{ii^*}\phi) = \frac{\partial \left(C_a D_{i^*}^0 \right)}{\partial C_a} (1 + K'_{i^*i^*}\phi) - C_a D_{i^*}^0 \phi \left(\frac{\partial K'_{ii^*}}{\partial C_a} \right)_{i=i^*} . \quad (A.7)$$

Differentiating the Stokes-Einstein equation, $D_{i^*}^0 = \frac{k_B T}{6\pi\eta R_{i^*}}$, one can show,

$$\frac{\partial \left(C_a D_{i^*}^0 \right)}{\partial C_a} = D_{i^*}^0 \left(1 - \frac{\partial ln R_{i^*}}{\partial ln C_a} \right) . \quad (A.8)$$

Combining eqs A.7 and A.8 yields,

$$\sum_{i=1}^{N} \frac{\partial \left(n_i D_i^0 \frac{C_s}{\overline{m}} \delta_{ii^*} \right)}{\partial C_a} (1 + K'_{ii^*}\phi) = D_{i^*}^0 \left\{ \left(1 - \frac{\partial ln R_{i^*}}{\partial ln C_a} \right) (1 + K'_{i^*i^*}\phi) - \phi \left(\frac{\partial K'_{ii^*}}{\partial ln C_a} \right)_{i=i^*} \right\} . \quad (A.9)$$

Now, focusing on the second summation on the right side of eq A.4, the derivative can be evaluated,

$$\sum_{i=1}^{N} n_i D_i^0 \frac{C_s}{\overline{m}} N_A V_i \delta_{ii^*} \frac{\partial}{\partial C_{\mathrm{a}}} \left\{ \left\{ \beta_{ii^*} \left(\frac{1+\lambda_{ii^*}}{2} \right)^3 + K''_{ii^*} \right\} \frac{C_s}{\overline{m}} \right\} = \sum_{i=1}^{N} n_i D_i^0 \frac{C_s}{\overline{m}} N_A V_i \delta_{ii^*} \frac{C_s}{\overline{m}} \left\{ \frac{3}{8} \beta_{ii^*} (1 + \lambda_{ii^*})^2 \left(\frac{\partial \lambda_{ii^*}}{\partial C_a} \right) + \left(\frac{1+\lambda_{ii^*}}{2} \right)^3 \left(\frac{\partial \beta_{ii^*}}{\partial C_a} \right) + \left(\frac{\partial K''_{ii^*}}{\partial C_a} \right) \right\} + \sum_{i=1}^{N} n_i D_i^0 \frac{C_s}{\overline{m}} N_A V_i \delta_{ii^*} \left\{ \beta_{ii^*} \left(\frac{1+\lambda_{ii^*}}{2} \right)^3 + K''_{ii^*} \right\} \frac{\partial}{\partial C_{\mathrm{a}}} \left(\frac{C_s}{\overline{m}} \right) , \quad (A.10)$$

and the sum over i is performed using the sifting property, $\phi = C_s/\bar{m}\, N_A V_{i^*}$, and $C_a = \bar{n}/\bar{m}\, C_s$:

$$\sum_{i=1}^{N} n_i D_i^0 \frac{C_s}{\bar{m}} N_A V_i \delta_{ii^*} \frac{\partial}{\partial C_\mathrm{a}} \left\{ \left\{ \beta_{ii^*} \left(\frac{1+\lambda_{ii^*}}{2} \right)^3 + K''_{ii^*} \right\} \frac{C_s}{\bar{m}} \right\} =$$

$$C_a D_{i^*}^0 \phi \left\{ \frac{3}{2} \beta_{i^* i^*} \left(\frac{\partial \lambda_{ii^*}}{\partial C_a} \right)_{i=i^*} + \left\{ \frac{\partial (\beta_{ii^*} + K''_{ii^*})}{\partial C_a} \right\}_{i=i^*} + (\beta_{i^* i^*} + K''_{i^* i^*}) \frac{\bar{m}}{C_s} \frac{\partial}{\partial C_\mathrm{a}} \left(\frac{C_s}{\bar{m}} \right) \right\} . \qquad (A.11)$$

The size ratio for spheres is defined as $\lambda_{ii^*} = \frac{R_{i^*}}{R_i}$. Hence,

$$\left(\frac{\partial \lambda_{ii^*}}{\partial C_a} \right)_{i=i^*} = \frac{\partial ln R_{i^*}}{\partial C_a} . \qquad (A.12)$$

Furthermore, since C_a and C_s are independent variables,

$$\frac{\bar{m}}{C_s} \frac{\partial}{\partial C_\mathrm{a}} \left(\frac{C_s}{\bar{m}} \right) = - \frac{\partial ln \bar{m}}{\partial C_\mathrm{a}} . \qquad (A.13)$$

Combining eqs A.11–A.13, one finds,

$$\sum_{i=1}^{N} n_i D_i^0 \frac{C_s}{\bar{m}} N_A V_i \delta_{ii^*} \frac{\partial}{\partial C_\mathrm{a}} \left\{ \left\{ \beta_{ii^*} \left(\frac{1+\lambda_{ii^*}}{2} \right)^3 + K''_{ii^*} \right\} \frac{C_s}{\bar{m}} \right\} =$$

$$D_{i^*}^0 \phi \left\{ \frac{3}{2} \beta_{i^* i^*} \frac{\partial ln R_{i^*}}{\partial ln C_a} + \left\{ \frac{\partial (\beta_{ii^*} + K''_{ii^*})}{\partial ln C_a} \right\}_{i=i^*} - (\beta_{i^* i^*} + K''_{i^* i^*}) \frac{\partial ln \bar{m}}{\partial ln C_\mathrm{a}} \right\} . \qquad (A.14)$$

Eqs A.4, A.9, and A.14 combine to yield

$$\frac{D_\mathrm{aa}}{D_{i^*}^0} = 1 + K'\phi - \left\{ 1 + \left(K' - \frac{3}{2}\beta \right) \phi \right\} \frac{\partial ln R_{i^*}}{\partial ln C_a} + \phi \left\{ \frac{\partial (\beta_{ii^*} + K''_{ii^*} - K'_{ii^*})}{\partial ln C_a} \right\}_{i=i^*} - (\beta + K'') \frac{\partial ln \bar{m}}{\partial ln C_\mathrm{a}} \phi . \qquad (A.15)$$

In eq A.15, redundant subscripts on the interaction coefficients have been removed. If the hydration index n_H is constant with composition, differentiation of eq 39 provides,

$$\frac{\partial ln \bar{m}}{\partial ln C_\mathrm{a}} = 3 \frac{\partial ln R_{i^*}}{\partial ln C_\mathrm{a}} - \frac{\phi_a}{\phi} , \qquad (A.16)$$

where $\phi_a = C_a N_A V_a$ is the solute volume fraction. Furthermore, if the interaction potential between pairs of micelles is, at most, a single variable function of the interparticle separation distance, then we may write,

$$\left\{ \frac{\partial (\beta_{ii^*} + K''_{ii^*} - K'_{ii^*})}{\partial ln C_a} \right\}_{i=i^*} = \left\{ \frac{d(K'' - K')}{d\lambda} \right\}_{\lambda=1} \left\{ \frac{\partial \lambda_{ii^*}}{\partial ln C_a} \right\}_{i=i^*} . \qquad (A.17)$$

Finally, eqs A.12 and A.15–A.17 combine, after some rearrangement, to produce,

$$\frac{D_\mathrm{aa}}{D_{i^*}^0} = 1 + K'\phi - M\left(\phi, \frac{C_a}{C_s} \right) , \qquad (A.18)$$

where the function $M\left(\phi, \frac{C_a}{C_s}\right)$ is given by,

$$M\left(\phi, \frac{C_a}{C_s} \right) = \frac{\partial ln R_{i^*}}{\partial ln C_a} (1 + \gamma\phi) - (\beta + K'')\phi_a , \qquad (A.19)$$

and

$$\gamma = \left(\frac{3}{2}\beta + K' + 3K'' \right) - \left\{ \frac{d(K'' - K')}{d\lambda} \right\}_{\lambda=1} . \qquad (A.20)$$

In order to determine the remaining elements of [**D**] in terms of $M\left(\phi, \frac{C_a}{C_s}\right)$, we note that R_{i^*} and $\bar{m}$ are thermodynamic state functions of a ternary solution. According to the Gibbs phase rule, these functions depend on four independent, intensive variables, which we choose to be T, p, C_a/C_s and ϕ. Our light scattering results[2] at constant T and p indicate R_{i^*} and $\bar{m}$ vary strongly with C_a/C_s but are weak functions of ϕ. Hence, to a good approximation, we may write expressions for R_{i^*} and $\bar{m}$ at constant T and p as a power series in C_a/C_s,

$$R_{i^*} = R_0 + \sum_{k=1}^{\infty} a_k \left(\frac{C_\mathrm{a}}{C_\mathrm{s}} \right)^k \qquad (A.21)$$

$$\bar{m} = m_0 + \sum_{k=1}^{\infty} b_k \left(\frac{C_\mathrm{a}}{C_\mathrm{s}} \right)^k . \qquad (A.22)$$

Differentiating equations A.21 and A.22 with respect to C_a and C_s, one finds,

$$\frac{\partial ln R_{i^*}}{\partial ln C_a} = - \frac{\partial ln R_{i^*}}{\partial ln C_s} \qquad (A.23)$$

$$\frac{\partial ln \bar{m}}{\partial ln C_a} = - \frac{\partial ln \bar{m}}{\partial ln C_s} . \qquad (A.24)$$

Eqs A.23 and A.24 may be used in derivations similar to that described above for D_aa to find

$$\frac{D_\mathrm{as}}{D_{i^*}^0} = \frac{C_a}{C_s} \left\{ (\beta + K'')\phi + M\left(\phi, \frac{C_a}{C_s} \right) \right\} \qquad (A.25)$$

$$\frac{D_\mathrm{sa}}{D_{i^*}^0} = - \frac{C_s}{C_a} M\left(\phi, \frac{C_a}{C_s} \right) \qquad (A.26)$$

$$\frac{D_\mathrm{ss}}{D_{i^*}^0} = 1 + (\beta + S)\phi + M\left(\phi, \frac{C_a}{C_s} \right) . \qquad (A.27)$$

In Table 1, exact numerical calculations by Batchelor[12,15] for the mobility coefficients K'_{ij} and K''_{ij} are provided for $\lambda_{ij} = 0.9$, 1.0, and 1.1. These numerical results were used to calculate the central difference approximation for the derivative, $\left\{ \frac{d(K'' - K')}{d\lambda} \right\}_{\lambda=1} = -4.70$, in eq A.20. Thus, for micelles that interact as identically sized ($\lambda = 1$) hard spheres, $\beta = 8$, $K' = -2.10$, $K'' = -4.45$, $S = K' + K'' = -6.55$, and $\gamma = 1.25$.

Table 1. Mobility coefficients calculated by Batchelor[12,15]

λ_{ij}	K'_{ij}	K''_{ij}
0.9	-2.13	-4.02
1.0	-2.10	-4.45
1.1	-2.06	-4.89

Appendix B: The solute tracer limit for [D]

Differentiation of eq A.21 provides

$$\frac{\partial lnR_{i^*}}{\partial lnC_a} = \frac{\sum_{k=1}^{\infty} k a_k \left(\frac{C_\mathrm{a}}{C_\mathrm{s}}\right)^k}{R_0 + \sum_{k=1}^{\infty} a_k \left(\frac{C_\mathrm{a}}{C_\mathrm{s}}\right)^k} \quad . \qquad (B.1)$$

Eq B.1 is divided by $C_\mathrm{a}/C_\mathrm{s}$ to yield

$$\frac{C_\mathrm{s}}{C_\mathrm{a}}\frac{\partial lnR_{i^*}}{\partial lnC_a} = \frac{a_1 + \sum_{k=2}^{\infty} k a_k \left(\frac{C_\mathrm{a}}{C_\mathrm{s}}\right)^{k-1}}{R_0 + \sum_{k=1}^{\infty} a_k \left(\frac{C_\mathrm{a}}{C_\mathrm{s}}\right)^k} \quad . \qquad (B.2)$$

Furthermore, we note that

$$\frac{C_\mathrm{s}}{C_\mathrm{a}}\frac{\phi_a}{\phi} = \frac{V_\mathrm{a}}{V_\mathrm{s} + n_\mathrm{H} V_\mathrm{w}} \quad . \qquad (B.3)$$

According to eqs B.1 and B.2, $\frac{\partial lnR_{i^*}}{\partial lnC_a} \to 0$ and $\frac{C_\mathrm{s}}{C_\mathrm{a}}\frac{\partial lnR_{i^*}}{\partial lnC_a} \to \frac{a_1}{R_0}$ in the limit as $\frac{C_\mathrm{a}}{C_\mathrm{s}} \to 0$. Hence, eqs 31–35 and B.1–B.3 combine to give,

$$\frac{D_{\mathrm{aa}}}{D^0} = 1 + K'\phi \qquad (B.4)$$

$$D_{\mathrm{as}} = 0 \qquad (B.5)$$

$$\frac{D_{\mathrm{sa}}}{D^0} = -\frac{a_1}{R_0}(1 + \gamma\phi) + (\beta + K'')\left(\frac{V_\mathrm{a}}{V_\mathrm{s} + n_\mathrm{H} V_\mathrm{w}}\right)\phi \qquad (B.6)$$

$$\frac{D_{\mathrm{ss}}}{D^0} = 1 + (\beta + S)\phi \,. \qquad (B.7)$$

Acknowledgements

This research was funded by the National Science Foundation (CBET1506474), and from Hatch project 1010420, from the USDA National Institute of Food and Agriculture. N. P. A. acknowledges a Jastro-Shields fellowship from the University of California at Davis.

References

1 Bird, R. B.; Stewart, W. E.; Lightfoot, E. N. *Transport Phenomena,* 2nd ed.; Wiley: New York, 2007.
2 Alexander, N. P.; Phillips, R. J.; Dungan, S. R. Multicomponent Diffusion in Aqueous Solutions of Nonionic Micelles and Decane. *Langmuir* **2019**, *35, 42,* 13595–13606.
3 Musnicki, W. J.; Dungan, S. R.; Phillips, R. J. Multicomponent Diffusion in Solute-Containing Micelle and Microemulsion Solutions. *Langmuir* **2014**, *30,* 11019−11030.
4 Leaist, D. G. Relating Multicomponent Mutual Diffusion and Intradiffusion for Associating Solutes. Application to Coupled Diffusion in Water-in-oil Microemulsions. *Phys. Chem. Chem. Phys.* **2002**, *4,* 4732–4739.
5 Budroni, M. A.; Carballido–Landeira J.; Intiso, A.; De Wit, A. Rossi, F. Interfacial Hydrodynamic Instabilities driven by Cross-Diffusion in Reverse Microemulsions. *Chaos* **2015**, *25,* 1−10.
6 Porat, D.; Dahan, A. Active Intestinal Drug Absorption and the Solubility–Permeability Interplay. *Int. J. Pharm.* **2018**, *537,* 84−93.
7 Miller J. M.; Beig, A.; Krieg, B. J.; Carr, R. A.; Borchardt, T. B.; Amidon, G. E.; Amidon, G. L.; Dahan, A. The Solubility–Permeability Interplay: Mechanistic Modeling and Predictive Application of the Impact of Micellar Solubilization on Intestinal Permeation. *Mol. Pharm.* **2011**, *8,* 1848−1856.
8 Zhang, H.; Annunziata, O. Modulation of Drug Transport Properties by Multicomponent Diffusion in Surfactant Aqueous Solutions. *Langmuir* **2008**, *24,* 10680–10687.
9 Everist, M.; MacNeil, J. A.; Moulins, J. R.; Leaist, D. G. Coupled Mutual Diffusion in Solutions of Micelles and Solubilizates. *Phys. Chem. Chem. Phys.* **2009**, *11,* 8173–8182.
10 Batchelor, G. K. Sedimentation in a dilute dispersion of spheres. *J. Fluid Mech.* **1972**, *52,* 245–268.
11 Batchelor, G. K. Sedimentation in a Dilute Polydisperse System of Interacting Spheres. Part 1. General Theory. *J. Fluid Mech.* **1982**, *119,* 379–408.
12 Batchelor, G. K.; Wen, C. S. Sedimentation in a Dilute Polydisperse System of Interacting Spheres. Part 2. Numerical Results. *J. Fluid Mech.* **1982**, *124,* 495–528.
13 Batchelor, G. K. Brownian Diffusion of Particles with Hydrodynamic Interaction. *J. Fluid Mech.* **1976**, *74,* 1–29.
14 Batchelor, G. K. Diffusion in a Dilute Polydisperse System of Interacting Spheres. *J. Fluid Mech.* **1983**, *131,* 155–175.
15 Batchelor, G. K. Corrigendum. *J. Fluid Mech.* **1983**, *137,* 467–469.
16 Russel, W. B.; Saville, D. A.; Schowalter, W. R. *Colloidal Dispersions;* Cambridge University Press, New York, 1st, 1989, 2, 21–63.
17 Taylor, G. I. Dispersion of Soluble Matter in Solvent Flowing Slowly through a Tube. *Proc. R. Soc. London, Ser. A.* **1953**, *219,* 186–203.
18 Aris, R. On the Dispersion of a Solute in a Fluid Flowing through a Tube. *Proc. R. Soc. London, Ser. A.* **1956**, *235,* 67–77.
19 Price, W. E. Theory of the Taylor Dispersion Technique for Three-component-system Diffusion Measurements. *J. Chem. Soc., Faraday Trans. 1* **1988**, *84,* 2431–2439.
20 Deng, Z.; Leaist, D. G. Ternary Mutual Diffusion Coefficients of $MgCl_2$ + $MgSO_4$ + H_2O and Na_2SO_4 + $MgSO_4$ + H_2O from Taylor Dispersion Profiles. *Can. J. Chem.* **1991**, *69,* 1548–1553.
21 Russo, V.; Ortona, O.; Tesser, R.; Paduano, L.; Di Serio, M. On the Importance of Choosing the Best Minimization Algorithm for Determination of Ternary Diffusion Coefficients by the Taylor Dispersion Method. *ACS Omega* **2017**, *2,* 2945−2952.
22 Berthod, A.; Tomer, S.; Dorsey, J. G. Polyoxyethylene Alkyl Ether Nonionic Surfactants: Physicochemical Properties and Use for Cholesterol Determination in Food. *Talanta*. **2001**, *55,* 69−83.
23 Massaldi, H. A.; Judson King, C.; Simple Technique to Determine Solubilities of Sparingly Soluble Organics: Solubility and Activity Coefficients of d–Limonene, n–Butylbenzene, and 7–Hexyl Acetate in Water and Sucrose Solutions. *J. Chem. Eng. Data.* **1973**, *18,* 393–397.
24 Tolls, J.; Dijk, J. V.; Verbruggen, E. J. M.; Hermens, J. L. M.; Loeprecht, B.; Schüürmann, G.; Aqueous Solubility–Molecular Size Relationships: a Mechanistic Case Study Using C_{10}- to C_{19}- Alkanes. *J. Phys. Chem. A* **2002**, *106,* 2760–2765.
25 Kirkwood, J. G.; Baldwin, R. L.; Dunlop, P. J.; Gosting, L. J.; Kegeles, G. Flow Equations and Frames of Reference for

Isothermal Diffusion in Liquids. *J. Chem. Phys*. **1960**, 33, 1505−1513

26 Hill, T. *An Introduction to Statistical Thermodynamics;* Addison-Wesley Publishing Company, Inc., United States, 2nd, 1960, 19, 340–368.

27 Banchio, A. J.; Nägele, G. Short-time Transport Properties in Dense Suspensions: From Neutral to Charge Stabilized Colloidal Spheres. *J. Chem. Phys*. **2008**, *128*, 104903.

28 Segre, P. N.; Behrend, O. P.; Pusey, P. N. Short-time Brownian motion in Colloidal Suspensions: Experiment and Simulation. *Phys. Rev. E.* **1995**, 52, 5, 5070–5083.

29 Ladd, A. J. C. Hydrodynamic Transport Coefficients of Random Dispersions of Hard Spheres. *J. Chem. Phys*. **1990**, *93*, 3484 – 3494.

30 Lindman, B.; Medronho, B.; Karlström, G. Clouding of Nonionic Surfactants. *Curr. Opin. Colloid Interface Sci*., **2016**, *22*, 23–29.

31 Zoeller, N.; Lue, L.; Blankschtein, D. Statistical-Thermodynamic Framework to Model Nonionic Micellar Solutions. *Langmuir*. **1997**, *13*, 5258–5275.

32 Vierros, S.; Sammalkorpi, M. Effects of 1-Hexanol on $C_{12}E_{10}$ Micelles: A Molecular Simulations and Light Scattering Study. *Phys. Chem. Chem. Phys*. **2018**, *20*, 6287–6298.

33 Glatter, O.; Fritz, G.; Lindner, H.; Brunner-Popela, J.; Mittelbach, R.; Strey, R.; Egelhaaf, S.U. Nonionic Micelles near the Critical Point: Micellar Growth and Attractive Interaction. *Langmuir*. **2000**, *16*, 8692– 8701.

34 Danino, D.; Talmon, Y.; Zana, R. Aggregation and Microstructure in Aqueous Solutions of the Nonionic Surfactant C12E8. *J. Colloid Interface Sci*. **1997**, *186*, 170–179.

35 Zulauf, M.; Weckstrom, K; Hayter, J. B.; Degiorgio, V.; Corti M. Neutron Scattering Study of Micelle Structure In Isotropic Aqueous Solutions of Poly(oxyethylene) Amphiphiles. *J. Phys. Chem*. **1985**, 89, 3411–3417.

36 Olsson, U.; Schurtenberger, P. Structure, Interactions, and Diffusion in a Ternary Nonionic Microemulsion Near Emulsification Failure. *Langmuir.* **1993**, *9*, 3389–3394.

37 Olsson, U.; Schurtenberger, P. A Hard Sphere Microemulsion. Progr. Colloid Polymer Sci. **1997**, *104*, 157–159.

38 Bernheim-Groswasser, A.; Wachtel, E.; Talmon, Y. Micellar Growth, Network Formation, and Criticality in Aqueous Solutions of the Nonionic Surfactant C12E5. *Langmuir*. **2000**, 16, 4131–4140.

39 Nagarajan, R.; Ruckenstein, E. Theory of Surfactant Self-Assembly: A Predictive Molecular Thermodynamic Approach. *Langmuir.* **1991**, *7,* 2934–2969.

40 Nagarajan, R. Constructing a Molecular Theory of Self-Assembly: Interplay of Ideas from Surfactants and Block Copolymers. *Adv. Colloid Interface Sci*. **2017**, *244*, 113−123.

41 Brady, J. F. The Long-time Self-diffusivity in Concentrated Colloidal Dispersions. *J. Fluid Mech.* **1994**, *212*, 109–133.

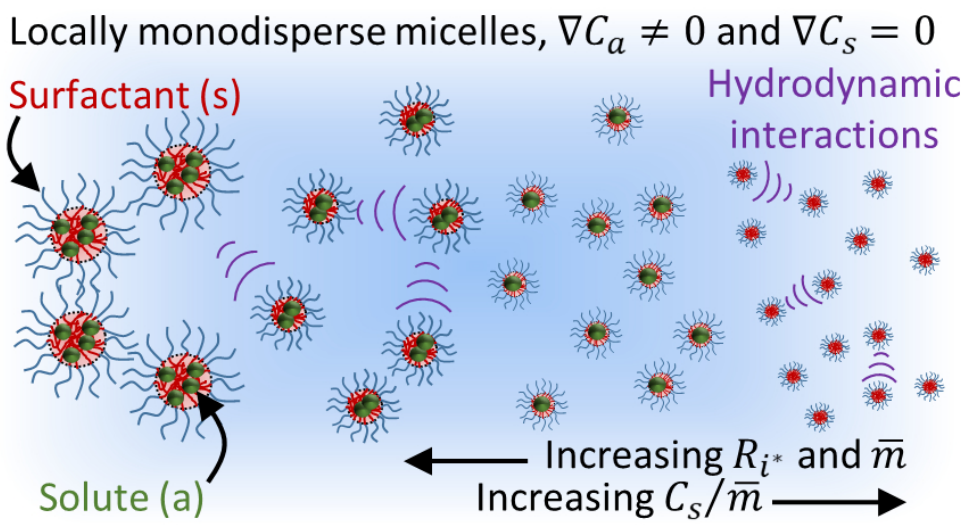

74x39mm (300 x 300 DPI)